AIMS Materials Science, 4(2): 452-469.
DOI: 10.3934/matersci.2017.2.452
Received: 30 December 2016
Accepted: 27 February 2017
Published: 03 March 2017

http://www.aimspress.com/journal/Materials

Research article

Inkjet printed drug-releasing polyelectrolyte multilayers for wound dressings

Huilin Yang and Amy M. Peterson *

Department of Chemical Engineering, Worcester Polytechnic Institute, 100 Institute Road, Worcester, Massachusetts 01609, USA

* **Correspondence:** Email: ampeterson@wpi.edu; Tel: 508-831-6029.

Abstract: Inkjet printing was used as a novel processing method for the preparation of polyelectrolyte multilayers. Conformal, consistent coatings were formed on a cotton substrate. As a demonstration of a potential application of this processing method, polyelectrolyte multilayers were assembled on cotton for wound dressing. When loaded with gentamicin, these coatings demonstrated burst release of 50% of the loaded gentamicin over the first five hours, followed by consistent release of 0.15 μg/(cm^2-h) for at least four days. Significant antimicrobial activity of the gentamicin-releasing polyelectrolyte multilayer-coated cotton was observed, with a zone of inhibition of 1.575 ± 0.03 cm. This result is comparable to the zone of inhibition for cotton soaked in gentamicin (1.75 ± 0.04 cm), indicating that the inkjet printing processing method does not degrade gentamicin. Inkjet printing shows promise as a low cost, versatile option for polyelectrolyte multilayer fabrication. Additionally, as a scalable process, inkjet printed samples exhibited consistent antibacterial function for over three months after preparation.

Keywords: polyelectrolyte multilayers; polyelectrolyte complexes; inkjet printing; Escheria coli; gentamicin; surface properties

1. Introduction

After damage to skin or after an operation, a wound is formed that will need to be healed. The process of wound healing relies on many phenomena over a range of length and time scales, include

inflammation, cell proliferation, and remodeling. This is a sensitive process that can be interrupted by disease, age, and infection. In the United States alone, approximately 6.5 million people suffer from chronic wounds, at an annual cost of $25 billion [1].

For serious skin damage, skin grafts and cell therapies are used to replace skin; however, less significant damage is treated with wound dressing, making wound dressing the most common approach to wound healing. Wound dressing is also the oldest wound healing treatment, and has been greatly improved by modern technologies. Hydrocolloid, alginate, hydrogel, foam, and biological dressings exhibit significant barrier properties and promote a moisture environment optimal for wound healing. These dressing materials can be further improved through the addition of active compounds, such as antimicrobial peptides (AMPs), microRNA, and antibiotics to promote healing [2–5].

Controlling the release of active compounds is crucial in medicated dressings. Controlled release could offer consistent drug delivery over long time periods and is more ideal for wound healing. Polymeric materials are often used as barriers to control the release of active compounds in wound dressings [6–13]. Polyelectrolytes, polymers with ionically dissociable repeat units, are a popular polymer choice for controlled release. The electrostatic interactions between the different charged groups can lead to the formation of polyelectrolyte complexes (PECs). One form of a polyelectrolyte complex is a polyelectrolyte multilayer (PEM), which is formed by alternating layer-by-layer (LbL) adsorption of a polycation and a polyanion. Since many polyelectrolytes have shown excellent biocompatibility, PEMs have been used in numerous biomedical applications. Examples include controlling cell transfection or differentiation [14,15], functionalization of living cells [16,17], fabrication of Janus particles for laser-assisted tissue welding [18,19], and delivery systems for biologically relevant molecules including antibiotics and anti-inflammatory drugs [20,21,22], lipophilic drugs [23,24,25], peptides [26,27,28], DNA and RNA [29,30,31], and growth factors [32–36].

PECs, including PEMs, have demonstrated outstanding antibacterial properties, making them good candidates for wound healing material [37–40]. PEC antibacterial strategies include preventing adhesion, contact killing and release killing. Polyelectrolytes generally prevent bacterial adhesion by having higher affinity for water, while stiffness can also be tuned to prevent adhesion. In addition, the positive charge and loading of bioactive compounds on the surface can also disturb bacterial proliferation and kill bacteria, or an antibacterial agent can be loaded within a PEC [37]. Bioactive cargoes, such as silver nanoparticles and chlorhexidine, and antiradical polycations, such as chitosan, have been incorporated within PEMs systems and impressive antibacterial performance and wound healing were reported [41,42,43]. PEMs are especially promising for heavily exuding wounds, which require efficient fluid absorbance as well as rehydration of dried wounds [44].

The most common method of PEM assembly is dip coating. In dip coating, the substrate is immersed in a polyelectrolyte solution for a set amount of time, followed by multiple rinses and immersion in a second polyelectrolyte solution of opposite charge. This process is repeated until the desired number of layers is achieved. There is very little equipment needed, consistent coatings can be achieved on complex shapes and while a significant volume of polyelectrolyte solution in which to dip the substrate is required, there is little waste [32,45]. In one example of dip-coated PEMs, Kirykhin et al. deposited PEMs via dip coating on a microchamber template, loaded the

microchambers, and transferred the PEM to a glass substrate [46,47]. Release from individual microchambers was achieved by a focused laser beam.

Other techniques include spray coating and spin coating. In a typical spray coating procedure, a polyelectrolyte is sprayed onto a substrate, followed by a rest/draining period, a washing period, an additional rest period, and repeating the cycle with a polyelectrolyte of the opposite charge. Spray coating is much faster than dip coating and can cover a larger surface area; however, it requires specialized equipment, is more wasteful than dip coating and results in non-uniform coating, with less material deposited on the edges of the spray plume. Schlenoff et al. estimate that 99% of the polyelectrolyte is rinsed off, while just 1% is adsorbed to the surface [48]. Spin coating is a highly controlled method for solution-based coating of a system. Spin coating of PEMs results in rapid, uniform coating, but is limited to small, flat substrates. Like spray coating, spin coating is more wasteful than dip coating. A typical spin coating procedure includes spin coating, rinsing by "spin coating" water and repeating the procedure with the oppositely charged polyelectrolyte [32,49,50].

Andres and Kotov previously applied inkjet printing to the assembly of LbL films of poly(diallydimethylammonium chloride) (PDADMAC) and gold nanoparticles (GNP) [51]. In order to achieve nanometer-scale layers without the need for rinsing, precise amounts of each component were delivered by using very low concentration solutions (0.0025 wt% PDADMAC and 2480 GNP/pL). In the current work, hybrid PEMs were assembled in a LbL fashion via a novel inkjet printing method. High concentration (15 mg/mL) polyelectrolyte solutions were used to prepare thick (~1 μm) conformal coatings. These are far thicker than coatings assembled via other methods, presumably because this method does not employ a rinse step. As a result, the reported coatings combine the assembly method of a PEM with the large thicknesses easily achievable from a PEC and represent a new, hybrid PEM. The resulting hybrid PEMs were used to load gentamicin within cotton paper, which acted as a model cotton-based wound dressing. Gentamicin is a broad-spectrum antibiotic with activity against many gram negative and some gram positive bacteria, and has been previously incorporated in PEM systems [20,52]. As a small, positively charged molecule with a broad anti-bacterial spectrum and similar structure to the chosen polyelectrolytes, gentamicin was also chosen as the antibiotic in this study. The physical, chemical, and antimicrobial properties of these coatings were characterized. It was found that the antimicrobial activity of gentamicin loaded within an inkjet printed PEM was maintained over long time periods.

2. Materials and Methods

2.1. Materials

PDADMAC solution (M_n ~ 200,000–350,000, 20 wt% in water), Poly(4-styrenesulfonic acid) solution (PSS, M_n ~ 75,000, 30 wt% in water), dimethyl sulfoxide (DMSO, ≥99.5%), o-phthaldialdehyde (≥99%), methanol (anhydrous, 99.8%), 2-mercaptoethanol (≥99.0%), sodium tetraborate (99%), 2-propanol (99.5%), gentamicin solution (50 mg/ml), Mueller Hinton Agar (MHA), and Mueller Hinton Broth (MHB) were obtained from Sigma-Aldrich. Formamide (99%), Diiodomethane (99%), and glycerol (>99%) were purchase from Alfa Aesar. Phosphate buffered saline tablets (PBS, pH = 7.4) were purchased from MP Biomedicals. 100% Pure Cotton Stationery

Paper was obtained from Strathmore and 122 HP Black Ink Cartridges were acquired from HP. *Escherichia coli* (*E. coli*) HB101 (ATCC 33694) were provided by Prof. Terri Camesano's lab. Unless otherwise noted, all materials were used as received.

2.2. PEM Coating Preparation

122 HP black ink cartridges were filled with PDADMAC and PSS solutions (15 mg/ml) separately after their filling sponges were removed and the cartridges were thoroughly rinsed and cleaned with DI water. A rectangle (13.3 cm long × 10.9 cm wide) was created in a word document and printed on cotton paper using PDADMAC and PSS solutions with a HP Deskjet 1000 Printer-J110a (Figure S1). Starting with PDADMAC solution, and alternating with PSS solution, rectangles were printed repetitively on the same piece of cotton paper multiple times to build PEMs. The paper was allowed to dry for 1–4 min between each printing. PEM-coated samples with 4.5, 5, 9.5, and 10 PDADMAC/PSS bilayers ($(PDADMAC/PSS)_{4.5}$, $(PDADMAC/PSS)_5$, $(PDADMAC/PSS)_{9.5}$, and $(PDADMAC/PSS)_{10}$ respectively) were printed and stored in a desiccator. Samples containing gentamicin were also produced. In that case, a gentamicin solution (15 mg/ml) was added to a third cleaned black ink cartridge. One layer of gentamicin was printed on the top of a sample coated with 10 bilayers ($(PDADMAC/PSS)_{10}$ + G, referred to as PEM + G) and uncoated cotton paper (Cotton + G). These samples were stored at 6 °C prior to testing.

2.3. Surface Characterization

The surface chemistry of PEM-coated cotton was characterized by FT-IR analysis. Dried samples with varying numbers of multilayers were measured using 64 scans on an FTIR Spectrometer Tensor 37 with pure cotton paper as background (BrukerOptics). Four positions on $(PDADMAC/PSS)_{10}$ were measured so as to evaluate the homogeneity of coated cotton. PDADMAC and PSS thin films were also tested using air as background, and results were compared with those of PEM-coated samples.

Contact angle analysis was performed using a contact angle goniometer (Ramé-Hart). The results were used to calculate surface energy of pure cotton paper, $(PDADMAC/PSS)_{9.5}$, and $(PDADMAC/PSS)_{10}$. For each kind of sample, 2 μL droplets of liquids with known surface energy were placed on a sample's surface and the resulting contact angles were recorded. At least five droplets per liquid were measured. For dried pure cotton paper water, glycerol, formamide, and diiodomethane were used; for PEM-coated samples, water, glycerol, formamide, ethanol and diiodomethane were used. Surface energies were directly determined by using the Owens-Wendt theory [53].

2.4. Gentamicin Release

Gentamicin release studies were conducted by immersing 1 × 1 cm^2 PEM + G ($(PDADMAC/PSS)_{10}$ + G) samples in PBS and storing them at 37 °C. 1 ml aliquots were regularly sampled. After each aliquot was taken the aliquot volume was immediately replaced with fresh PBS.

All aliquots were immediately refrigerated at 6 °C. Release from five samples was measured for each time point.

Gentamicin release was quantified based on a protocol developed by Cabanillas et al. and Tan et al. [54,55]. Briefly, an o-phthaldialdehyde reagent solution was made 24 h before use by dissolving 0.25 g o-phthaldialdehyde in 6.25 ml methanol, 0.3 ml 2-captoethanol, and 56 ml of a sodium borate solution (0.04 M). The resulting solution was stored in a brown bottle at 6 °C prior to use. 1.5 ml testing samples were made by mixing 0.5 ml each of the o-phthaldialdehyde reagent, isopropanol and a collected aliquot or PBS solution. The testing samples were incubated at room temperature for exactly 30 min before collecting spectra. All testing was performed with a UV-VIS Evolution 300 Spectrometer (Thermo Scientific). PBS was used as the background. The peak absorbance was recorded from the range of wavelengths from 331 nm to 333 nm. A calibration curve of absorbance with known concentrations of gentamicin was generated using the same method.

To study the effectiveness of PEMs as a reservoir for controlled release of gentamicin, ten 0.635 cm diameter circular PEM + G and Cotton + G samples (twenty samples total) were prepared. Five PEM + G and five Cotton + G samples were immersed in 1 ml PBS solutions individually. The other samples were immersed in 10 ml PBS individually. 1 ml aliquots of each release medium were collected after 24 h immersion. All aliquots were immediately stored at 6 °C and were tested for gentamicin concentrations as described above.

Release kinetics was analyzed in order to better understand the release mechanism. The Higuchi model, developed in 1961 and derived from Fick's first law of diffusion, is widely used to describe the release of drugs from a solid matrix, and has been previously used to describe release from PEMs and hydrogels under specific conditions [56,57]. Its basic form can be written as:

$$M_t = A\sqrt{D(2C_0 - C_S)C_S t} \tag{1}$$

where M_t is the cumulative amount of drug released at time t, A is the surface area from which the drug is released, D is the Fickian drug diffusivity within the system, C_0 is the initial drug concentration in the matrix and C_S is the solubility of the drug in the system. This equation can easily be reduced to a simpler form:

$$\frac{M_t}{M_\infty} = K\sqrt{t} \tag{2}$$

where M_∞ is the cumulative amount of drug released at infinite time and K is a constant reflecting the design variables of the system. Since the Higuchi model describes transport as a function of the square root of time, it is only valid for the first 60% of the total drug release [58].

2.5. Antimicrobial Activity Assay

A Zone of Inhibition (ZOI) study was used as an assay for antimicrobial activity of PEM + G, Cotton + G, PEM, and bare cotton paper. *E. coli* were cultured in 9 ml ½ standard concentration MHB at least for 12 h at 37 °C. 100 µl of the bacteria solution was extracted from the culture and added to a fresh 9 ml ½ standard concentration MHB and incubated at 37 °C for an additional 8 h.

The concentration of fresh bacteria culture was corrected to 0.5 McFarland standard, and the solution was evenly coated on MHA plates. For the initial ZOI studies, circular samples (diameter = 0.635 cm) of PEM + G, Cotton + G, PEM, and bare cotton paper placed on the prepared plates. To evaluate longer term antimicrobial activities, circular samples were immersed individually in 10 mL PBS solutions for at least 24 h and placed on the prepared plates. Plates were incubated at 37 °C for at least for 12 h. Diameters of inhibited zones (including sample's diameter) were measured and recorded.

3. Results and Discussion

3.1. Inkjet Printing of Hybrid PEMs

Hybrid PEMs were assembled on cotton paper using an inkjet printer, as described in Section 2.2. Cotton paper was selected as a model substrate, since many traditional wound dresses are cotton based due to cotton's excellent absorbing ability. PDADMAC and PSS are common strong polyelectrolytes, and their PEMs have been previously used to encapsulate small molecules, such as dextran, as well as peptides [7,28]. As such, PDADMAC/PSS PEMs were seen as a good candidate for an antimicrobial agent reservoir.

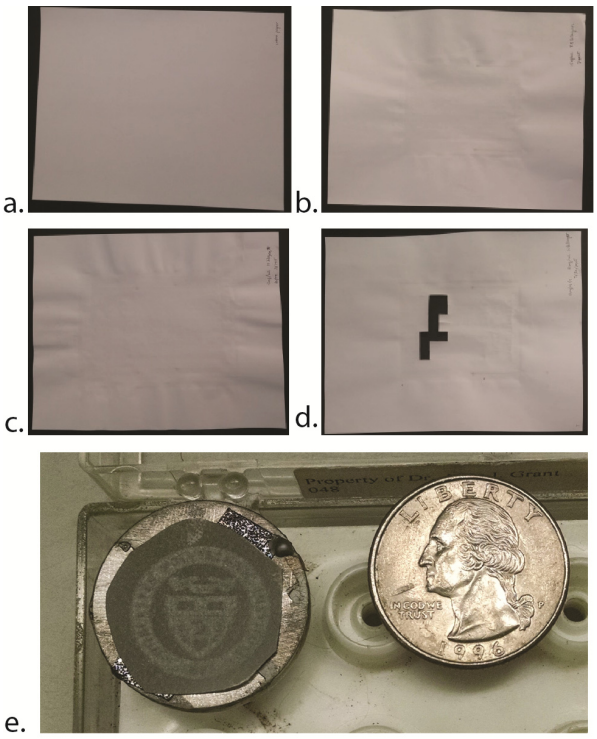

Figure 1. Examples of printed PEMs. a) Uncoated cotton paper; b) $(PDADMAC/PSS)_{9.5}$; c) $(PDADMAC/PSS)_{10}$; d) $(PDADMAC/PSS)_{10}$ + G. Samples have been cut from the center of the $(PDADMAC/PSS)_{10}$ + G coated paper for further analysis. Each sheet is 21.6 cm × 27.9 cm. e) $(PDADMAC/PSS)_{10}$ printed in the shape of WPI's logo and gold sputter coated. Quarter (diameter = 2.43 cm) included for scale.

Examples of the resulting samples are shown in Figure 1. A ten bilayer system could be assembled in less than three hours. While there is some warping along the edges of the printed area, the paper could still be printed upon with ease. This technique is versatile: different shapes can be printed, different numbers of layers in various locations are possible, and chemistry can be adjusted by changing the cartridge. To explore the printed coatings further, SEM images were collected (Figure 2). Inkjet printed PEMs conformally coat the cotton paper. In some cases, the coating stretches between cotton fibers (Figure 2d and 2f).

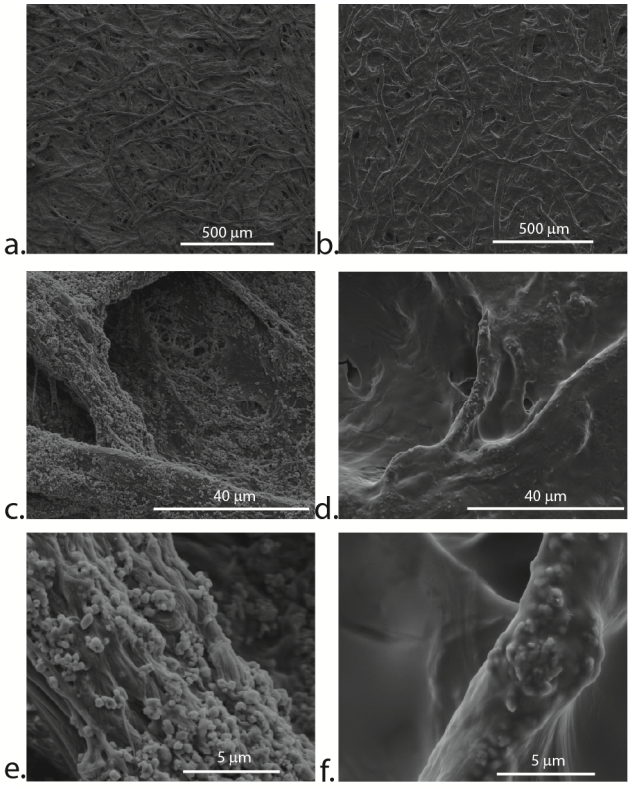

Figure 2. SEM of uncoated (a, c, e) and coated (b, d, f) cotton paper at different magnifications. Coated cotton paper is coated with $(PDADMAC/PSS)_{10}$.

Typically, PEM growth is on the order of 1–10 nm per bilayer, with growth rate increasing with solution ionic strength [59,60]. These solutions have low ionic strength (0.073 M for PSS and 0.064 M for PDADMAC), so we would expect that ten bilayers would be at 10–100 nm thick. However, in comparing Figures 2e and 2f it is clear that the thickness of the printed coating is ~1 µm thick. This difference in thickness is due to the lack of a rinse step in the processing, which allows loosely bound polyelectrolytes to remain in the system. As a result, the PEC formed is a hybrid PEM, with thicker layers and a structure that may be more homogeneous through the thickness thanks to the loosely bound polyelectrolyte that remains on the surface after layer deposition.

Entropy is the driving force for PEC assembly, since electrostatic interactions between polyanions and polycations release counterions, causing an increase in the system's entropy [59]. However, the hybrid PEMs prepared in this study were assembled without a rinse step and high

concentration solutions are used. Entropy is still the driving force in the chemical interactions within the hybrid PEM, but gravity and diffusion also play important roles in assembly.

3.2. PEM Surface Characterization

The chemistry of hybrid PDADMAC/PSS PEMs on cotton paper and its consistency were characterized using ATR-FTIR. Since ATR-FTIR penetrates to a depth of a few microns, the collected spectra should average across the entire PEM and into the substrate. Spectra were collected from four locations on the printed surface of a $(PDADMAC/PSS)_{10}$ sample and are shown in Figure 3. Characteristic peaks corresponding to PDADMAC and PSS are observed at 2920 cm^{-1} and 1037 cm^{-1}, respectively [61]. These results confirm that PDADMAC and PSS are present on the cotton surface. The spectra in Figure 3 shows identical peak locations; however, ratio of the magnitude of the peak at 3500 cm^{-1} and the trough at 3280 cm^{-1} vary. The broad peak at 3500 cm^{-1} corresponds with a hydrogen bonded O–H stretch, which would be consistent with water that is hydrogen bonded within the PEM [62]. The trough at 2380 cm^{-1} corresponds with a peak in the cotton paper background that is correlated with intermolecular and intramolecular hydrogen bonding in cotton [63]. There is an inverse relationship between the magnitude of the peak and trough, i.e., more absorbance of the PEM-related peak means more absorbance (less of a lack of absorbance) of the cotton-related peak. This could be caused by some samples having incomplete contact with the ATR crystal. In general, these results indicate that cotton is uniformly coated by the printing process.

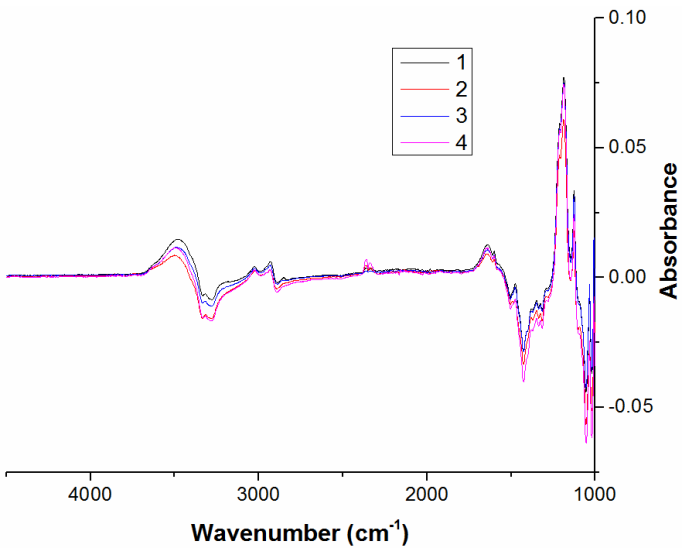

Figure 3. ATR-FTIR of four locations on cotton paper inkjet printed with $(PDADMAC/PSS)_{10}$. Cotton paper is used as the background.

Surface energies for cotton and cotton paper with different numbers of PEM bilayers were calculated from static contact angle measurements. Results are shown in Figure 4. Total surface energies are very close for the 9.5 and 10 bilayer coated cotton; however, the coating with PSS as the top layer (10 bilayers) has a larger polar component than the coating with PDADMAC as the top

layer. These results run counter to the asymmetric growth of PDADMAC/PSS PEMs previously reported, wherein PDADMAC overcompensates the charge of PSS and PSS merely compensates PDADMAC charge, and lend further evidence that inkjet printed PEMs more closely resemble PECs than traditional nanoscale PEMs [60]. Significant differences between the 9.5 and 10 bilayer conditions can also be seen in the static contact angle data (Figure S2). In particular, differences were observed between water and formamide contact angles on different substrates.

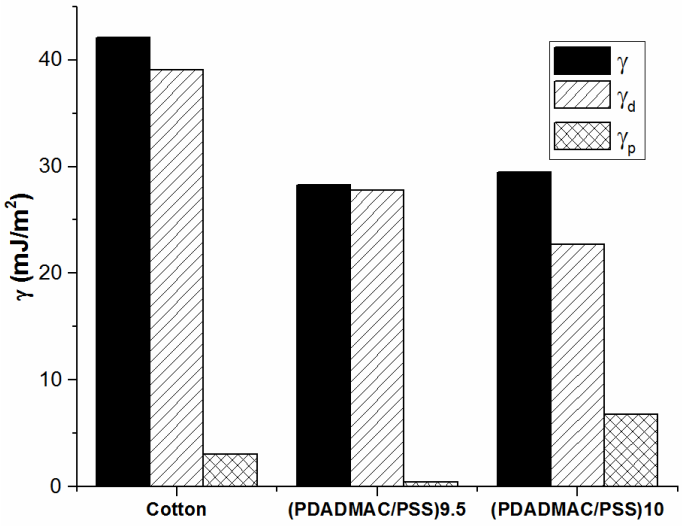

Figure 4. Surface free energy of cotton paper and cotton coated with 9.5 and 10 bilayers of PDADMAC/PSS PEM. Solid bar is total surface free energy, lined bar is the dispersive component of surface energy, hatched bar is the polar component of surface energy.

3.3. Gentamicin Release

Release of gentamicin from inkjet printed PEMs is shown in Figure 5. The majority of release (46% of what is loaded) occurs in the first five hours. These rates are not representative of the case of topical application, however, since release studies were performed under highly mobile conditions. It is anticipated that, in a wound setting, release would be slower. Overall, 65.2 ± 4.0 μg/cm^2 gentamicin is released from $(PDADMAC/PSS)_{10}$ + G over the course of 103 hours (4.3 days), which is longer than the recommended treatment duration for gentamicin of 48 hours [64]. This amount is comparable to gentamicin release from hydrolytically degradable PEMs with 50 tetralayers (200 layers) [55].

Two zones of release are observed in Figure 5. The first zone corresponds to burst release, a common phenomenon in drug release profiles in polymeric systems. Although burst release has been observed for numerous PEMs, the underlying mechanisms are still poorly understood. Parameters that may influence diffusion include the substrate surface properties, the morphology and porosity of the PEM coating as well as the processing conditions [11]. In the experiments reported here, the immersion of the samples into the release medium could be the main cause of the observed burst

release, since the PEM coatings swell as water diffuses between the polymer chains [65]. This swelling causes chain reorganization, breaking electrostatic bonds and forming new ones as a hybrid PEM structure is achieved that is more loosely bound than before due to its hydration. This less dense PEM, along with faster transport due to the presence of water molecules in the multilayer, would greatly promote the diffusion of gentamicin. Moreover, a concentration gradient would be established between the gentamicin-rich PEM and the gentamicin-free medium in which the sample is immersed, resulting in osmosis, which would further increase the release rate. The rate of gentamicin release is substantially slower than previously reported from PEMs, which can be attributed to the thicker hybrid PEM coating [66].

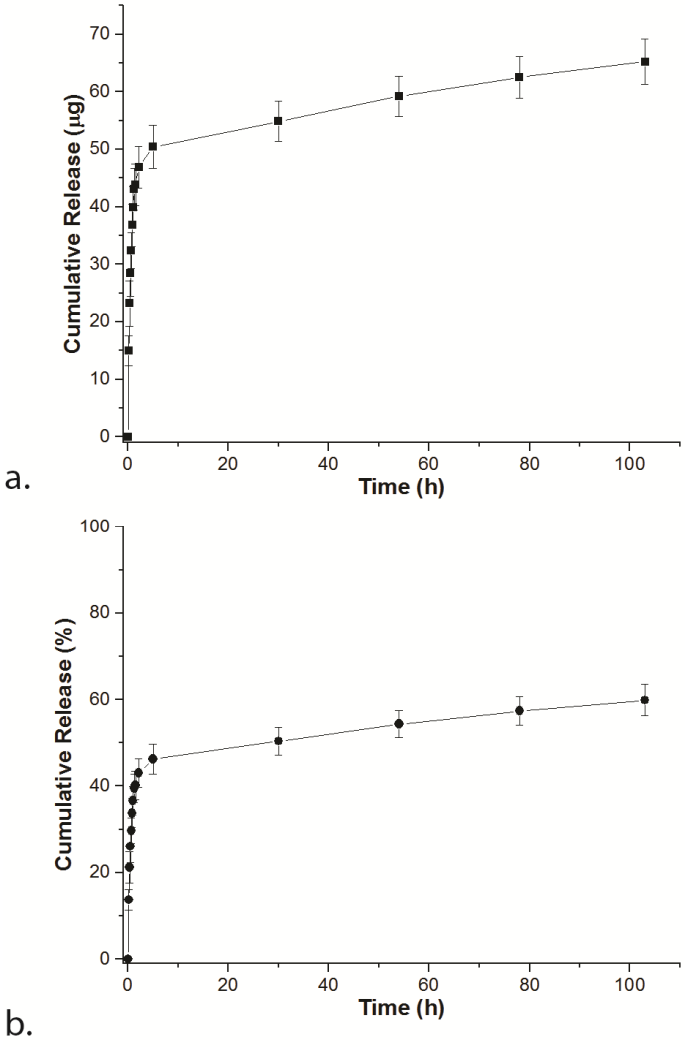

Figure 5. Cumulative release of gentamicin from $(PDADMAS/PSS)_{10}$+G based on a. amount and b. percent loaded. Error bars represent standard deviation.

The second regime presents a fairly linear profile ($R^2 = 0.936$) after the initial burst release. The transition to this regime occurs when steady-state diffusion is reached after completion of the PEM swelling and reorganization. Linear release is observed in this system after 1 h of release, which is on

the same time scale as PEM reorganization that was previously observed via quartz crystal microbalance with dissipation monitoring (QCM-D). However, it is much faster than the time scale for swelling, which was observed to occur over days [67].

Although a depletion regime has been previously described for growth factor release from PEMs, it was not observed in this study [67]. The amount of gentamicin release, as compared to the amount loaded into the coating, is less than 60% over the time period investigated. Gentamicin has been shown to be stable for at least 15 days at 37 °C, indicating that reason for incomplete recovery of gentamicin is not degradation [68]. Gentamicin is a charged molecule, so it can electrostatically bind with the PEM coating, which would prolong the time for full release and could prevent complete release.

Gentamicin release kinetics was further explored to learn more about the release mechanism. Salvi et al. previously reported that Fickian and Higuchi release behavior do not sufficiently describe growth factor release from PEMs [67]. Since the Higuchi model assumes that the polymer phase does not swell or degrade during the diffusion process and Fickian diffusion is better suited to describe the diffusion of small, uncharged molecules instead of charged macromolecules with complex secondary structure, this result was not surprising. However, gentamicin is a small molecule and PDADMAC/PSS swelling or degradation may be less significant, particularly in the shorter release times for this study. Therefore, there is value in comparing the data in Figure 5 to the Higuchi equation.

The data obtained during release studies were plotted and fitted to the Higuchi model for all points, since the amount of release is less than 60% of the amount loaded, and the Higuchi model is valid for the first 60% of total drug release. Poor agreement with the Higuchi model was observed over the whole time period ($R^2 = 0.707$); however, data agreed well with the Higuchi model over the first 1.5 hours ($R^2 = 0.9765$), which is close to the transition from burst to steady-state release.

Berg et al. found that the zero-order model (constant release rate) was consistent with complete drug release profiles for PEM systems [69]; however, in most cases a zero-order model has been reported to only be representative of later stage in the release process [20,57]. From Figure 5, it can be concluded that the Higuchi model describes early stage release well, while a zero-order model describes release at later times. Siepmann and Peppas reported that the increased plasticity of the multilayer caused by hydration of the polymer matrix can enhance molecule transport through a case-II mechanism [70]. The phenomena of diffusion through the PEM, transport induced by dynamic swelling, and physical degradation of the PEM should be all taken into account in order to devise an accurate model of drug release from PEMs. However, in this instance, simple relationships can be used to describe release and indicate that secondary interactions do not play a significant role in the release mechanism.

3.4. Antimicrobial Activity

The antimicrobial activity of gentamicin-releasing coatings was evaluated against *E. coli*. Infection of surgical wounds is commonly caused by *E. coli*. Zone of inhibition (ZOI) measurements were recorded for gentamicin-loaded $(PDADMAC/PSS)_{10}$ inkjet printed on cotton (PEM + G), as well as three controls: cotton paper (Cotton), cotton paper soaked in gentamicin (Cotton + G), and

$(PDADMAC/PSS)_{10}$ inkjet printed on cotton (PEM). Results are summarized in Figure 6 and example plates are shown in Figure 7. Only the gentamicin containing samples showed any ZOI. While the gentamicin-releasing PEM showed a similar level of antimicrobial activity to cotton paper soaked in gentamicin, the Cotton + G condition was statistically significantly different from all other conditions ($p < 0.01$). A potential reason that Cotton + G was the best performing condition could be that more gentamicin was loaded. Alternatively, gentamicin could be released more rapidly or in greater amounts from Cotton + G than PEM + G. PEMs have been previously shown to decrease the rate of release of drugs and other biologically relevant molecules, with thicker coating sustaining release to a greater extent [32,37].

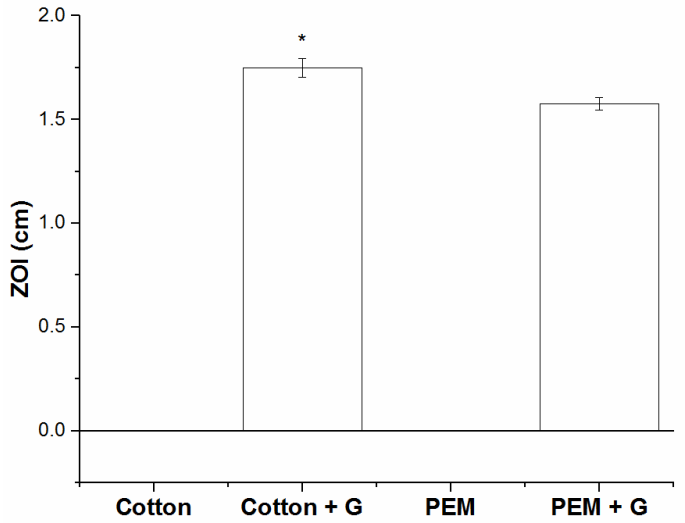

Figure 6. ZOI of gentamicin-releasing PEMs and controls (cotton, cotton soaked in gentamicin, and PEM). Error bars represent standard deviations, * = $p < 0.01$.

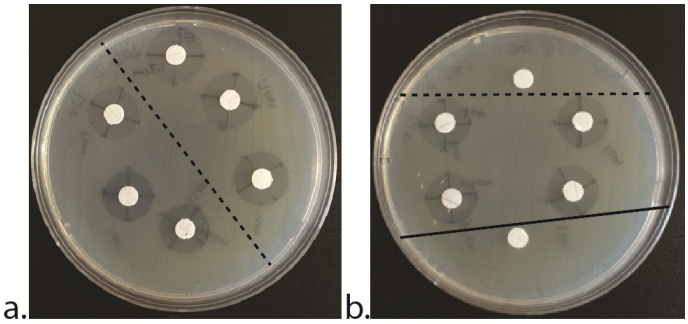

Figure 7. Example plates after 12 h of *E. coli* culture. a) Cotton + G to right of dashed line, PEM + G to left of dashed line; b) Cotton above dashed line, PEM + G in the middle, PEM below solid line.

To explore the question of PEM + G antimicrobial activity further, PEM + G and Cotton + G samples were immersed individually in 10 mL PBS for 24 hours at 37 °C. The amount of gentamicin

release was measured as 53.7 ± 14.1 μg/cm^2 and 50.3 ± 4.1 μg/cm^2 for PEM + G and Cotton + G, respectively. These difference between these quantities is not statistically significant ($p = 0.63$). With these results in mind, the difference in performance between PEM + G and Cotton + G does not result from different amounts of gentamicin released. The most likely reason for the statistically significantly different ZOI is that the PEM is more favorable to *E. coli* growth than uncoated cotton, perhaps because the terminating layer of the PEM is a polyanion or because the polycation selected is not as inherently antibacterial as polyelectrolytes with NH_3^+ groups [37,40].

After immersion, the samples were cultured in the presence of *E. coli* and ZOI measurements were recorded. Both PEM + G and Cotton + G showed zones of inhibition (0.72 ± 0.041 and 0.84 ± 0.029 cm, respectively). Cotton + G again exhibited a higher ZOI ($p < 0.01$), supporting the conclusion that the PEM is more favorable to *E. coli* growth than uncoated cotton.

Gentamicin stability within the PEM was evaluated by comparing antimicrobial activity of PEM + G to freshly prepared Cotton + G over more than three months. The results, which are shown in Figure 8, demonstrate that the PEM + G antimicrobial activity does not change significantly, even after 100 days of storage. This is a very promising result for larger scale fabrication of PEM-coated wound dressings, since antimicrobial activity is maintained over long time periods.

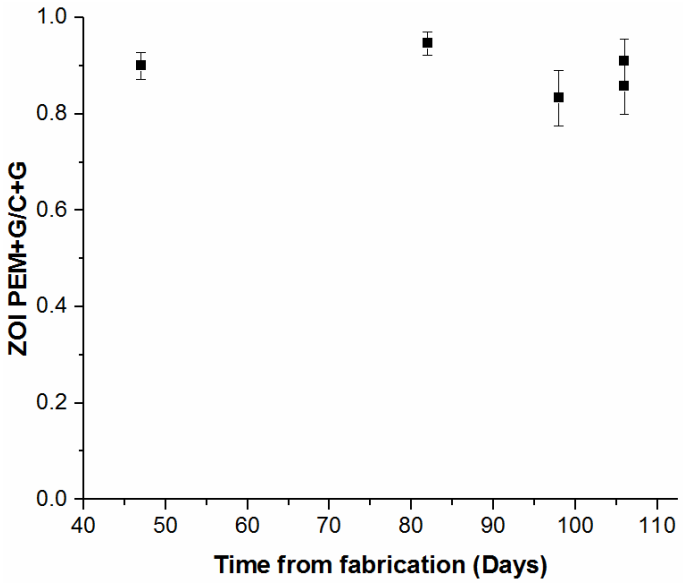

Figure 8. Ratio of ZOI for gentamicin-releasing PEMs to ZOI for cotton paper soaked in gentamicin as a function of time from PEM + G fabrication. All Cotton + G samples were prepared the day of culture. Error bars represent relative error.

4. Conclusions

Conformal PEM coatings were assembled via inkjet printing on cotton. These coatings could then be loaded with gentamicin. While PEM-coated cotton did not display any antimicrobial activity, PEM-coated cotton loaded with gentamicin display significant antimicrobial activity that could be maintained for over 100 days. A burst of gentamicin was released over the first five hours, followed

by steady release for the next four days. This system shows promise for wound dressing applications. Future work will focus on strategies for improving the PEM's base antimicrobial activity, including different polycation/polyanion pairs, terminating layers, and assembly conditions. Inkjet printing of polyelectrolyte multilayers is also being investigated for other flexible substrate applications, including electronics and stimuli-responsive materials.

Acknowledgements

The authors are particularly grateful for Prof. Terri Camesano and Lindsay Lozeau for providing *E. coli* and for the use of the Camesano lab microbial cell culture facilties. The authors also acknowledge Prof. Chris Lambert for use of the contact angle goniometer and Prof. Arne Gericke for use of the FTIR.

Conflict of Interest

All authors declare no conflicts of interest in this paper.

References

1. Sen CK, Gordillo GM, Roy S, et al. (2009) Human skin wounds: A major and snowballing threat to public health and the economy. *Wound Repair Regen* 17: 763–771.
2. Mangoni ML, Mcdermott AM, Zasloff M (2016) Antimicrobial peptides and wound healing: Biological and therapeutic considerations. *Exp Dermatol* 25: 167–173.
3. Fahs F, Bi X, Yu FS, et al. (2015) New insights into microRNAs in skin wound healing. *IUBMB Life* 67: 889–896.
4. You HJ, Han SK (2014) Cell therapy for wound healing. *J Korean Med Sci* 29: 311–319.
5. Boateng JS, Matthews KH, Stevens HNE, et al. (2008) Wound healing dressings and drug delivery systems: A review. *J Pharm Sci* 97: 2892–2923.
6. Zelikin AN (2010) Drug Releasing Polymer Thin Films: New Era of Surface-Mediated Drug Delivery. *ACS Nano* 4: 2494–2509.
7. Delcea M, Möhwald H, Skirtach AG (2011) Stimuli-responsive LbL capsules and nanoshells for drug delivery. *Adv Drug Deliver Rev* 63: 730–747.
8. Kataoka K, Harada A, Nagasaki Y (2001) Block copolymer micelles for drug delivery: design, characterization and biological significance. *Adv Drug Deliver Rev* 47: 113–131.
9. Qiu Y, Park K (2001) Environment-sensitive hydrogels for drug delivery. *Adv Drug Deliver Rev* 53: 321–339.
10. Yamada Y, Harashima H (2008) Mitochondrial drug delivery systems for macromolecule and their therapeutic application to mitochondrial diseases. *Adv Drug Deliver Rev* 60: 1439–1462.
11. Huang X, Brazel CS (2001) On the importance and mechanisms of burst release in matrix-controlled drug delivery systems. *J Control Release* 73: 121–136.
12. Kost J, Langer R (2001) Responsive polymeric delivery systems. *Adv Drug Deliver Rev* 46: 125–148.

13. Wohl BM, Engbersen JFJ (2012) Responsive layer-by-layer materials for drug delivery. *J Control Release* 158: 2–14.
14. Meyer F, Dimitrova M, Jedrzejenska J, et al. (2008) Relevance of bi-functionalized polyelectrolyte multilayers for cell transfection. *Biomaterials* 29: 618–624.
15. Lee IC, Wu YC (2014) Assembly of Polyelectrolyte Multilayer Films on Supported Lipid Bilayers To Induce Neural Stem/Progenitor Cell Differentiation into Functional Neurons. *ACS Appl Mater Inter* 6: 14439–14450.
16. Fakhrullin RF, Zamaleeva AI, Minullina RT, et al. (2012) Cyborg cells: functionalisation of living cells with polymers and nanomaterials. *Chem Soc Rev* 41: 4189–4206.
17. Fakhrullin RF, Lvov YM (2012) "Face-Lifting" and "Make-Up" for Microorganisms: Layer-by-Layer Polyelectrolyte Nanocoating. *ACS Nano* 6: 4557–4564.
18. He W, Frueh J, Shao J, et al. (2016) Guidable GNR-Fe_3O_4-PEM@SiO_2 composite particles containing near infrared active nanocalorifiers for laser assisted tissue welding. *Colloid Surface A* 511: 73–81.
19. He W, Frueh J, Hu N, et al. (2016) Guidable Thermophoretic Janus Micromotors Containing Gold Nanocolorifiers for Infrared Laser Assisted Tissue Welding. *Adv Sci* 3: 1600206.
20. Moskowitz JS, Blaisse MR, Samuel RE, et al. (2010) The effectiveness of the controlled release of gentamicin from polyelectrolyte multilayers in the treatment of Staphylococcus aureus infection in a rabbit bone model. *Biomaterials* 31: 6019–6030.
21. Shukla A, Fang JC, Puranam S, et al. (2012) Release of vancomycin from multilayer coated absorbent gelatin sponges. *J Control Release* 157: 64–71.
22. Shukla A, Fuller RC, Hammond PT (2011) Design of multi-drug release coatings targeting infection and inflammation. *J Control Release* 155: 159–166.
23. Teng XR, Shchukin DG, Möhwald H (2008) A Novel Drug Carrier: Lipophilic Drug-Loaded Polyglutamate/Polyelectrolyte Nanocontainers. *Langmuir* 24: 383–389.
24. Shchukina EM, Shchukin DG (2011) LbL coated microcapsules for delivering lipid-based drugs. *Adv Drug Deliver Rev* 63: 837–846.
25. González-Toro DC, Ryu JH, Chacko RT, et al. (2012) Concurrent binding and delivery of proteins and lipophilic small molecules using polymeric nanogels. *J Am Chem Soc* 134: 6964–6967.
26. Shukla A, Fleming KE, Chuang HF, et al. (2010) Controlling the release of peptide antimicrobial agents from surfaces. *Biomaterials* 31: 2348–2357.
27. Huang Y, Luo Q, Li X, et al. (2012) Fabrication and in vitro evaluation of the collagen/hyaluronic acid PEM coating crosslinked with functionalized RGD peptide on titanium. *Acta Biomater* 8: 866–877.
28. Palankar R, Skirtach AG, Kreft O, et al. (2009) Controlled intracellular release of peptides from microcapsules enhances antigen presentation on MHC class I molecules. *Small* 5: 2168–2176.
29. Zhang J, Chua LS, Lynn DM (2004) Multilayered thin films that sustain the release of functional DNA under physiological conditions. *Langmuir* 20: 8015–8021.
30. Kim SH, Jeong JH, Lee SH, et al. (2008) Local and systemic delivery of VEGF siRNA using polyelectrolyte complex micelles for effective treatment of cancer. *J Control Release* 129: 107–116.

31. Cho HJ, Chong S, Chung SJ, et al. (2012) Poly-L-arginine and dextran sulfate-based nanocomplex for epidermal growth factor receptor (EGFR) siRNA delivery: its application for head and neck cancer treatment. *Pharm Res* 29: 1007–1019.
32. Magboo R, Peterson AM (2016) Polyelectrolyte multilayers for controlled release of biologically relevant molecules. In: Somasundaran P, *Encyclopedia of Surface and Colloid Science*, Taylor and Francis, 1519–1533.
33. Shah NJ, Macdonald ML, Beben YM, et al. (2011) Tunable dual growth factor delivery from polyelectrolyte multilayer films. *Biomaterials* 32: 6183–6193.
34. Crouzier T, Ren K, Nicolas C, et al. (2009) Layer-by-layer films as a biomimetic reservoir for rhBMP-2 delivery: Controlled differentiation of myoblasts to osteoblasts. *Small* 5: 598–608.
35. Peterson AM, Pilz-Allen C, Kolesnikova T, et al. (2014) Growth factor release from polyelectrolyte-coated titanium for implant applications. *ACS Appl Mater Inter* 6: 1866–1871.
36. Gand A, Hindié M, Chacon D, et al. (2014) Nanotemplated polyelectrolyte films as porous biomolecular delivery systems: Application to the growth factor BMP-2. *Biomatter* 4: e28823.
37. Seon L, Lavalle P, Schaaf P, et al. (2015) Polyelectrolyte Multilayers: A Versatile Tool for Preparing Antimicrobial Coatings. *Langmuir* 31: 12856–12872.
38. Grunlan JC, Choi JK, Lin A (2005) Antimicrobial behavior of polyelectrolyte multilayer films containing cetrimide and silver. *Biomacromolecules* 6: 1149–1153.
39. Lichter JA, Van Vliet KJ, Rubner MF (2009) Design of Antibacterial Surfaces and Interfaces: Polyelectrolyte Multilayers as a Multifunctional Platform. *Macromolecules* 42: 8573–8586.
40. Gomes AP, Mano JF, Queiroz JA, et al. (2012) Layer-by-Layer Deposition of Antibacterial Polyelectrolytes on Cotton Fibres. *J Polym Environ* 20: 1084–1094.
41. Agarwal A, Nelson TB, Kierski PR, et al. (2012) Polymeric multilayers that localize the release of chlorhexidine from biologic wound dressings. *Biomaterials* 33: 6783–6792.
42. Yang JM, Yang JH, Huang HT (2014) Chitosan/polyanion surface modification of styrene-butadiene-styrene block copolymer membrane for wound dressing. *Mater Sci Eng C* 34: 140–148.
43. Dai J, Bruening ML (2002) Catalytic Nanoparticles Formed by Reduction of Metal Ions in Multilayered Polyelectrolyte Films. *Nano Lett* 2: 497–501.
44. Rieger KA, Birch NP, Schiffman JD (2013) Designing electrospun nanofiber mats to promote wound healing—a review. *J Mater Chem B* 1: 4531.
45. Wood KC, Chuang HF, Batten RD, et al. (2006) Controlling interlayer diffusion to achieve sustained, multiagent delivery from layer-by-layer thin films. Proceedings of the National Academy of Sciences, 103: 10207–10212.
46. Kiryukhin MV, Man SM, Tonoyan A, et al. (2012) Adhesion of polyelectrolyte multilayers: Sealing and transfer of microchamber arrays. *Langmuir* 28: 5678–5686.
47. Kiryukhin MV, Gorelik SR, Man SM, et al. (2013) Individually addressable patterned multilayer microchambers for site-specific release-on-demand. *Macromol Rapid Comm* 34: 87–93.
48. Schlenoff JB, Dubas ST, Farhat T (2000) Sprayed Polyelectrolyte Multilayers. *Langmuir* 16: 9968–9969.
49. Patel PA, Dobrynin AV, Mather PT (2007) Combined effect of spin speed and ionic strength on polyelectrolyte spin assembly. *Langmuir* 23: 12589–12597.

50. Kiel M, Mitzscherling S, Leitenberger W, et al. (2010) Structural characterization of a spin-assisted colloid-polyelectrolyte assembly: stratified multilayer thin films. *Langmuir* 26: 18499–18502.
51. Andres CM, Kotov NA (2010) Inkjet deposition of layer-by-layer assembled films. *J Am Chem Soc* 132: 14496–14502.
52. Schmidt DJ, Moskowitz JS, Hammond PT (2011) Electrically Triggered Release of a Small Molecule Drug from a Polyelectrolyte Multilayer Coating. *Chem Mater* 22: 6416–6425.
53. Owens DK, Wendt RC (1969) Estimation of the surface free energy of polymers. *J Appl Polym Sci* 13: 1741–1747.
54. Frutos Cabanillas P, Diez Pena E, Barrales-Rienda JM, et al. (2000) Validation and in vitro characterization of antibiotic-loaded bone cement release. *Int J Pharmaceut* 209: 15–26.
55. Tan H, Peng Z, Li Q, et al. (2012) The use of quaternised chitosan-loaded PMMA to inhibit biofilm formation and downregulate the virulence-associated gene expression of antibiotic-resistant staphylococcus. *Biomaterials* 33: 365–377.
56. Peterson AM, Pilz-Allen C, Möhwald H, et al. (2014) Evaluation of the role of polyelectrolyte deposition conditions on growth factor release. *J Mater Chem B* 2: 2680–2687.
57. Liu TY, Lin YL (2010) Novel pH-sensitive chitosan-based hydrogel for encapsulating poorly water-soluble drugs. *Acta Biomater* 6: 1423–1429.
58. Siepmann J, Peppas NA (2001) Modeling of drug release from delivery systems based on hydroxypropyl methylcellulose (HPMC). *Adv Drug Deliver Rev* 48: 139–157.
59. von Klitzing R (2006) Internal structure of polyelectrolyte multilayer assemblies. *Phys Chem Chem Phys* 8: 5012–5033.
60. Ghostine RA, Markarian MZ, Schlenoff JB (2013) Asymmetric growth in polyelectrolyte multilayers. *J Am Chem Soc* 135: 7636–7646.
61. Schoeler B, Sharpe S, Hatton TA, et al. (2004) Polyelectrolyte multilayer films of different charge density copolymers with synergistic nonelectrostatic interactions prepared by the layer-by-layer technique. *Langmuir* 20: 2730–2738.
62. Armstrong G, Buggy M (2005) Hydrogen-bonded supramolecular polymers: A literature review. *J Mater Sci* 40: 547–559.
63. Abidi N, Hequet E, Cabrales L (2011) Applications of Fourier transform infrared spectroscopy to study cotton fibers, In: Nikolic G, *Fourier Transforms—New Analytical Approaches and FTIR Strategies*, InTech, 90–114.
64. Moulds RFW, Jeyasingham MS (2010) Gentamicin: A great way to start. *Aust Prescr* 33: 35–37.
65. Schönhoff M, Ball V, Bausch AR, et al. (2007) Hydration and internal properties of polyelectrolyte multilayers. *Colloid Surface A* 303: 14–29.
66. Hu N, Frueh J, Zheng C, et al. (2015) Photo-crosslinked natural polyelectrolyte multilayer capsules for drug delivery. *Colloid Surface A* 482: 315–323.
67. Salvi C, Lyu X, Peterson AM (2016) Effect of assembly pH on polyelectrolyte multilayer surface properties and BMP-2 release. *Biomacromolecules* 17: 1949–1958.
68. Schafer T, Pascale A, Shimonaski G, et al. (1972) Evaluation of gentamicin for use in virology and tissue culture. *Appl Microbiol* 23: 565–570.

69. Berg MC, Zhai L, Cohen RE, et al. (2006) Controlled drug release from porous polyelectrolyte multilayers. *Biomacromolecules* 7: 357–364.
70. Siepmann J, Peppas NA (2011) Higuchi equation: derivation, applications, use and misuse. *Int J Pharmaceut* 418: 6–12.

AIMS Press